2000

Design and simulation of continuous scintillator with pixellated photodetector

G. J. Takacs
University of Wollongong, gjt@uow.edu.au

Anatoly B. Rosenfeld
University of Wollongong, anatoly@uow.edu.au

M. L. Lerch
University of Wollongong, mlerch@uow.edu.au

S. W. Lindsay
University of Melbourne

G. N. Taylor
University of Melbourne

See next page for additional authors

Design and Simulation of Continuous Scintillator with Pixellated Photodetector. [1]

G.J. Takacs[2], *Member IEEE*, A.B. Rosenfeld[2], *Senior Member IEEE*, M.L.F. Lerch[2], *Member IEEE*, S.W. Lindsay[3], G.N. Taylor[3], S.R Meikle[4], *Member IEEE*, S. Eberl[4], *Member IEEE*, and V.L. Perevertailo[5].
[2]Centre for Medical Radiation Physics, University of Wollongong, NSW, 2522, Australia
[3]High Energy Physics Department, University of Melbourne, Vic., Australia
[4]PET and Nuclear Medicine Department, Royal Prince Alfred Hospital, Sydney, N.S.W. Australia
[5]SPA "Detector", Ukraine.

Abstract

We present results of simulations performed as part of the development of a gamma-ray detector module comprising a non-pixellated scintillator and pixellated photodiode detector. The simulations have been carried out to determine the effect of surface treatment and dimensions of the scintillator on the ability to determine the 2-D position of interaction. A set of 32 different combinations of surface treatments have been considered for each crystal size. Scintillator dimensions considered have been 25 mm x 25 mm x(3-6 mm). For scintillator thicknesses at the low end of this range, an average accuracy of 0.5 to 0.6 mm is achievable for many different surface treatments. At the higher end of the thickness range, 6 mm, the average accuracy reduces to around 0.7 mm, and is more dependent on the surface treatment.

I. Introduction

During the last decade the combination of scintillator-silicon photodetectors (PD) are finding increasing applications in nuclear medicine instrumentation, particularly in mammography [1] and PET detector modules [2]. Such applications have been made possible due to essential improvements in PD quality (low noise, improved spectral sensitivity between the wavelength region 420-600 nm), development of multichannel readout CMOS single chips [3,4] and availability of pixellated scintillators [1]. However, pixellated scintillators in conjunction with silicon pixel PDs demand light isolation between each pixel, which reduces the efficiency of the detector due to the reduction in size of the scintillator pixel. The aim of present development is to investigate the possibility of 3D detection of position of interaction (POI) of the gamma photon in a non-pixellated scintillator crystal optically attached to silicon pixel PD array. Such detectors could then be used as the basis of SPECT and PET detector modules that are independent of photomultiplier tubes.

The silicon arrays to be used consist of 64 photodiodes, each 3 mm by 3 mm, in a square array 25 mm long. These are to be coupled, using optical grease, to one face of a scintillator crystal, of area 25 mm x 25 mm, with thicknesses from 3 to 6 mm. The remaining surfaces of the scintillator crystal may be covered with diffuse or specular reflectors. The modules as described could then be used edge on, with most of the gamma rays entering through a 25 mm x 3 mm face, or front on with the gamma rays entering primarily through the face opposite the diode array. Two materials have been considered for the scintillator, CsI(Tl) or LSO. These are very different in terms of their light output (both spectral content and amount), attenuation coefficient, and their decay times, but have very similar refractive indices. These parameters are summarised in Table 1 [5,6].

Table 1
Scintillator Propertiess

Property	LSO	CsI(Tl)
Refractive Index	1.82	1.79
Attenuation for 511keV	0.88 cm^{-1}	0.45 cm^{-1}
e-h pairs for 511 keV	9 300	20 000

For the proposed detector modules, it is important that the dimensions and surface treatment of the scintillator crystals are chosen to maximize the resolution of the detector. The detector resolution is determined by the ability to calculate, from the signals of the photodiode array, the coordinates of the point of interaction of the gamma ray in the crystal. Thus it is desirable to have a simulation code which enables i) the study of the light propagation in the scintillator and how the detected light is distributed between the pixels of the photodiode array, and ii) uses this light distribution to the calculate the point of interaction of the gamma ray in the scintillator. In the past many people have used Monte Carlo codes to study the propagation of light in scintillator crystals, however, due to our quite specific requirements it was decided to develop our own code. The simulations performed for this paper are similar in one respect to those of Siegel et al., [6], using the DETECT program, in that we create a pixel image of the light distribution on the detector surface. However, we do so here for the specific purpose of calculating the 2-D interaction position and determining how the accuracy of this calculation varies with surface treatment.

II. Description of Detector Module

The 25 mm x 25 mm silicon 8x8 PD was developed in collaboration with SPA "Detector". Each 3 mm x 3 mm PD has low noise level (reverse current of 0.1 nA at full depletion) and energy resolution for 662 keV gamma photons of 8 % with CsI(Tl) and 23 %with LSO [7].

[1]This work supported by Department of Industry, Science and Resources, Australia, and National Health and Medical Research Council, Australia, grant number 980493.

0-7803-6503-8/01/$10.00 2001 IEEE

In contrast to other developments [8], our design of n-Si pixel PD allows for the attachment of a 25 mm x 25 mm scintillator crystal on the p^+ side of the PD. The aim of this design is to enhance the time properties of the detector module in coincidence mode, due to the fast hole collection near the surface of the p^+ region.

For imaging applications, the parallel readout of all pixels is required. The signal output pads of the pixel PD have a 90 micron pitch and are all located on one side of PD, allowing easy connection to a VIKING readout chip. VIKING is a high speed 128 channel chip designed for strip detectors used in high energy physics (HEP) applications and is well known [4]. The low rms noise of about 150 electrons for several picofarads input capacitance of each pixel, and low cost, together with its proven ability in the application of data acquisition used in HEP vertex detectors, make this chip attractive for medical imaging instrumentation. The limitation of the PD pixel size in such design is due to the S/N, which depends not just on the pixel capacitance and reverse bias leakage current, but also on the number of photons reaching the pixel element and noise of electronics.

III. Simulations of Light Distribution

A. *Description of the Simulation Code*

The simulation code we have developed has two main functions. The first is to simulate the transport of scintillation light photons in the scintillator, and the second is to calculate the interaction position.

To simulate the propagation of scintillation light in the crystal we generate a specified number of photons, at a point in the crystal, with randomly chosen directions with uniform probability per unit solid angle. The point of intersection of the photon trajectory and the scintillator surface is determined and the surface conditions are then used along with the Fresnel relations for unpolarised light to determine the reflection probability and scattered direction. We have not considered scattering or attenuation of light within the crystal volume.

Surfaces are treated as either rough or smooth. The treatment of reflection used in the code essentially follows that used by Bea et al., [8], and is similar to that in DETECT97 [9,10]. Rough surfaces are described using a facet model, with a Gaussian distribution of slopes of standard deviation equal to the rms slope. This is slightly different to the model in DETECT97 where the angles of the facets are assumed to follow a Gaussian distribution. However, for small rms slopes the models will be equivalent. Another difference with DETECT97 is that we have not implemented any of the spike or lobe constants described as part of the UNIFIED model of reference [10].

Surfaces may be specified as being clad with a diffuse reflective material, specular reflector, detectors, or uncovered. For diffuse reflection, we have assumed Lambert's law so that the probability for reflection at an angle θ to the surface normal is independent of incident angle and proportional to $sin2\theta d\theta$. A small air gap is assumed to exist between the scintillator and any cladding material.

Each photon is followed until it exits the scintillator plus any cladding. If a photon exits on the detector surface the count for the diode it enters is incremented. After the selected number of photons have left the scintillator the code calculates the x and y coordinates of the point of the gamma ray interaction using the number of photons incident on the photodiodes plus any noise.

Photodiode noise and its effects are simulated by adding to the counts for each photodiode a random number of counts, specified by an r.m.s. value, varying between r.m.s./2 and 3x r.m.s./2 with a triangular distribution. We have assumed a noise figure of 200 r.m.s.

Various algorithms have been trialled for calculating the POI. These include; i) doing polynomial fits to the diode counts along two orthogonal lines of diodes through the maximum position, ii) modified Anger logic, iii) using the highest diode and all neighbouring diodes, and iv) linear combinations of the coordinates of the diode centre for the n highest diodes. In this latter case we have also tried weighting the diode coordinates both proportionally to the number of photons incident on each diode and proportionally to the square of the number incident on the diode. Of the four approaches, the final method is consistently and significantly better than the others and all POI results presented in this paper are for the final method. While a full discussion of the results from these algorithms is outside the scope of the present paper, it is worth noting that when the scintillator surfaces are rough, the quadratic weighting of diode coordinates gives a significantly better result than a first order weighting. If all surfaces are smooth, however, then the two weighting schemes give about the same result (in terms of the magnitude of the error in POI). We have also found that the best results are obtained when n = 4, that is only the four highest diode counts are used.

Output from the code consists of: i) the coordinates of each scintillator photon incident on the photodiode array, ii) the number of photons incident on each photodiode, iii) the x and y coordinates of the interaction point, iv) the calculated x and y coordinates of the interaction point using various algorithms, and v) the error between the calculated and actual gamma ray position of interaction in the xy plane for the respective algorithm.

An example showing the number of photons incident on each diode in an 8x8 photodiode detector array is given in Figure 1. The crystal surfaces are unclad and smooth and the total number of scintillator photons generated was 25,000. The noteworthy feature from this figure is that about 60 percent of detected photons are in four bins.

The simulations reported here have been carried out using a refractive index of 1.8 for the scintillator. This value is close to that for both CsI and LSO. Outside all surfaces, except the detector surface, the refractive index has been taken as 1.0, while on the detector surface a value of 1.5 has been assumed. We make the assumption that any photon exiting through the top surface is absorbed in the detector. For all the simulations

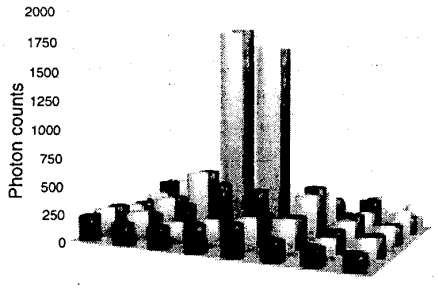

Figure 1: Distribution of detected photons plus noise for interaction point in the centre of scintillator

reported here, unless stated otherwise, 25 000 photons have been generated at each gamma ray interaction point. This value is about the number to be expected for 511 keV gammas incident on CsI scintillators. When cladding has been specified, it has been assumed to have a reflectivity of 0.95.

B. Surface Treatment Effects

In order to examine the effect of surface treatment on the accuracy of determination of the 2-D POI the simulation code was used as follows for each set of surface conditions. First, a point is generated at random within the volume of the crystal. After the specified number of photon histories, noise is added to each diode count and the diode counts are used to calculate the 2-D POI and the magnitude of the difference between the real 2-D POI and the calculated 2-D POI (the error). This process is carried out for one thousand randomly chosen interaction points, and the average error is then calculated. This process is repeated for a total of 32 combinations of surface treatments.

The results of this are summarised in Table2 for crystals of dimensions 25x25x3 mm and 25x25x6 mm. In this table, top refers to the detector surface, "s"means the surface was smooth, "r" means the surface was rough, "u" means uncovered while "c" means clad with a diffuse reflector. All rough surfaces in this table were modelled as having facets with slopes of standard deviation equal to one, which is quite rough. The column labelled output gives the percent of generated photons which exit the top (detector) surface. The error is the average error over the 1000 points randomly selected within the crystal and is in mm and in all cases has been calculated using a weighted average of the coordinates of the four highest diodes. By repeating these simulations with different seeds for the random number generator, we have determined the 95% confidence level in 2-D POI errors to be 0.02 mm and 0.1% for the light output. The letter "l" next to the error indicates a first order weighting, while "q" denotes a second order or quadratic weighting.

From these results it is quite clear that for the 3mm thick crystal, the surface treatment has only a small effect on the accuracy. This is despite there being quite a large variation in the light output for different surface treatments. However, for the 6 mm thick crystal there is a pronounced variation. For both

Table 2
Dependence of 2-D POI accuracy on surface treatment

Surface					Thickness 3 mm		Thickness 6 mm	
Sides		Bottom		Top	Output	Error	Output	Error
s	u	s	u	s	37.3	0.64 (l)	37.3	0.86 (q)
s	u	s	u	r	54.4	0.61 (l)	49.3	0.79 (q)
s	u	s	c	s	44.2	0.52 (l)	44.2	0.66 (q)
s	u	s	c	r	61.2	0.53 (l)	56.0	0.59 (q)
s	u	r	u	s	51.6	0.61 (l)	46.7	0.75 (q)
s	u	r	u	r	52.1	0.57 (l)	45.4	0.72 (q)
s	u	r	c	s	61.9	0.56 (l)	56.3	0.72 (q)
s	u	r	c	r	61.2	0.55 (l)	53.6	0.65 (q)
s	c	s	u	s	37.3	0.62 (q)	37.3	0.90 (q)
s	c	s	u	r	86.5	0.63 (q)	75.3	0.85 (q)
s	c	s	c	s	44.2	0.55 (l)	44.2	0.72 (q)
s	c	s	c	r	94.4	0.54 (l)	91.2	0.67 (q)
s	c	r	u	s	79.0	0.61 (q)	76.0	0.79 (q)
s	c	r	u	r	81.0	0.57 (q)	78.8	0.73 (q)
s	c	r	c	s	94.3	0.57 (q)	91.2	0.71 (q)
s	c	r	c	r	95.1	0.56 (q)	92.6	0.68 (q)
r	u	s	u	s	56.9	0.66 (q)	54.2	1.01 (q)
r	u	s	u	r	61.3	0.65 (q)	54.4	1.00 (q)
r	u	s	c	s	67.8	0.62 (q)	65.0	0.76 (q)
r	u	s	c	r	71.2	0.59 (q)	64.6	0.78 (q)
r	u	r	u	s	57.7	0.66 (q)	52.0	0.89 (q)
r	u	r	u	r	59.3	0.65 (q)	52.2	0.94 (q)
r	u	r	c	s	70.6	0.61 (q)	63.5	0.81 (q)
r	u	r	c	r	70.9	0.61 (q)	62.7	0.80 (q)
r	c	s	u	s	81.3	0.75 (q)	80.2	1.25 (q)
r	c	s	u	r	84.3	0.67 (q)	81.4	1.24 (q)
r	c	s	c	s	96.0	0.67 (q)	95.6	0.91 (q)
r	c	s	c	r	96.9	0.62 (q)	95.9	0.90 (q)
r	c	r	u	s	78.6	0.67 (q)	77.1	1.02 (q)
r	c	r	u	r	80.2	0.67 (q)	78.3	1.02 (q)
r	c	r	c	s	96.6	0.62 (q)	95.6	0.93 (q)
r	c	r	c	r	96.8	0.62 (q)	95.7	0.91 (q)

thicknesses, whether the top surface is rough or smooth seems to have little effect. When we compare the results for smooth sides to those for rough sides, it is clear that smooth sides are marginally better for the 3mm thickness and significantly better for 6 mm thickness, despite there being less light collected than for rough sides. Quite clearly, treating the surface to increase the light output is not necessarily the best course to follow.

Another significant feature from these results is that cladding the surface opposite the detector array (bottom) improves the accuracy. This improvement is significantly more pronounced for the thicker crystal, and appears to be slightly more pronounced when the detector surface (top) itself is smooth. It is also noteworthy that the best result for the 6 mm thick crystal, an average accuracy of 0.59 mm, is not significantly worse than that for the 3 mm thick crystal of 0.52 mm.

C. *Positional Variability*

In this section we examine the dependence of the error in the 2-D POI on the location of the POI in the scintillator, for the 3 mm thick case. In the previous section we determined the average error in the 2-D POI for a large number of points generated at random throughout the entirety of the scintillator. In practice, any application of this detector module is unlikely to result in gamma ray interaction points with a uniform distribution . Here we determine the average error for points randomly located within restricted volumes in the scintillator. There are two cases to consider. First, how does the error depend on distance from the edge, and secondly, how does the error depend on distance from the detector surface?

To examine the dependence of the 2-D POI error on distance from the edge of the scintillator we have used the code to generate 1000 interaction points at random, uniformly distributed throughout a restricted volume of the scintillator. The distance of the centre this volume from the edge of the crystal is then varied. This has been carried out for the third combination of surface conditions listed in Table 2. The volume used was 3 mm high (the full thickness of the scintillator), 0.78125 mm wide (one quarter of the diode to diode spacing) and 3.125 mm long. The position of this volume was moved from one edge of the scintillator, directly under one of the central rows of diodes, toward the centre of the scintillator. Figure 2 below shows the results obtained. Clearly, the error throughout most of the crystal is much lower than for interaction points located near the edge. Thus, for applications where the gamma rays are approaching from the edge of the module and hence are more likely to interact near the edge, it will be necessary to either develop a more sophisticated algorithm for the POI calculation, or modify the design of the module, if the average errors given in the previous section are to be achieved.

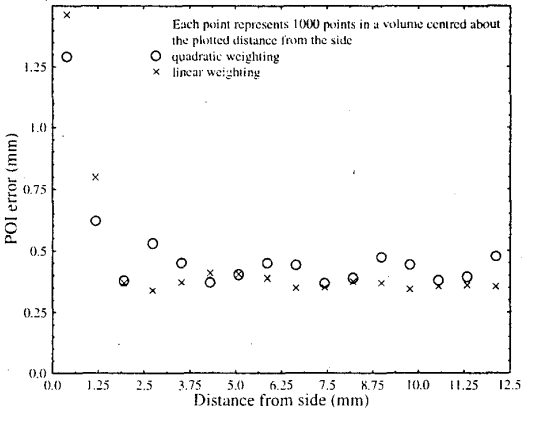

Figure 2: Dependence of POI error on distance from side of crystal.

The second case to be examined is the dependence of the 2-D POI error on distance from the detector surface. To look at this we have considered volumes 25 mm x 25 mm x 0.3 mm and used 1000 interaction points throughout this volume. The average error for the 1000 points has been determined for 10 such volumes and is plotted in Figure 3 below as a function of average distance from the detector surface. This has been done for two POI algorithms, using linear weighting of the four highest bin coordinates, and also using quadratic weighting.

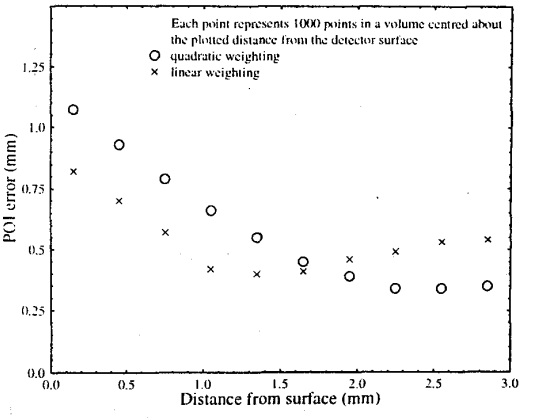

Figure 3: Dependence of POI error on distance from detector surface.

Clearly, both algorithms give their worst results for points located near the detector plane, with the linear weighting giving a lower error here than the quadratic. Near the surface opposite the detector surface, the quadratic weighting gives the better result. Therefore, for applications where the gamma rays would be entering through the surface opposite the detector surface it would be better to use the quadratic weighting.

D. *z Dependence of Light Distribution*

Thus far no mention has been made of extracting information about the z coordinate of the POI. This requires a more exacting analysis of the light distribution over the detector plane than is needed to extract the x-y information. In particular, what is needed is knowledge of how the light distribution varies as a function of distance from the detector plane, and whether this variation may be reliably inferred from the 8 x 8 pixel map that we have of it.

In Figure 4 we compare one dimensional profiles, through the two dimensional light distribution, for three different distances from the detector plane. These have been produced from 100 x 100 pixel maps and are for a scintillator 3 mm thick with all surfaces smooth and unclad. Remembering that for our 8 x 8 array the spacing between diode centres is 3.125 mm, it is clear that for the 3mm thick crystal we never get more than about 2 diodes width for our light distribution.

The linear dependence of the FWHM with distance from the detector is shown in Figure 5. This is for interaction points with x and y coordinates placing them in the middle of the crystal. The determination of the z coordinate of the point of interaction is thus reduced to determining the FWHM from the 8 x 8 pixel map of the light distribution. In Figure 6 we show the distribution for an interaction point 2.7 mm from the detector surface and with x and y coordinates in the middle of the scintillator. This light distribution is not significantly different from that displayed in Figure 1, despite there being a

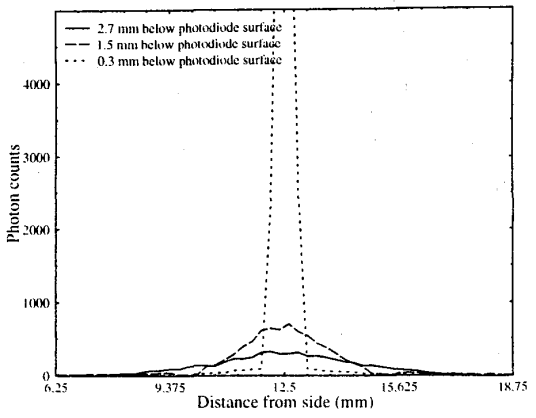

Figure 4: Profiles through the light distribution for three different distances from the detector plane

difference in the z coordinate of 1.2 mm. It appears then that extraction of the z coordinate from this light distribution will, if at all possible, be a considerable challenge.

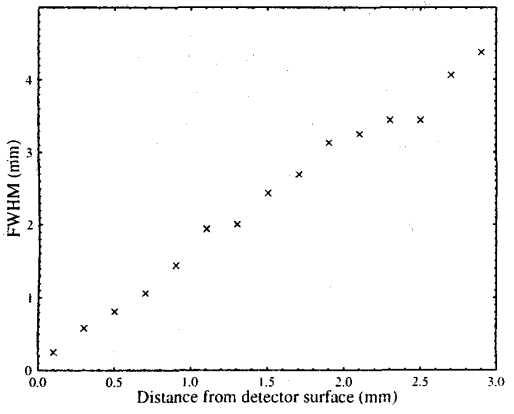

Figure 5: Dependence of FWHM on distance from detector surface for points in middle of scintillator

IV. Conclusions

We have shown that with our design of gamma ray detector module it should be possible to measure the 2-D POI to around 0.5 mm accuracy. This figure could be reduced by improving the accuracy of this calculation for interactions occurring near the sides of the scintillator and near the detector surface. Further work also needs to be done on methods of reliability estimating the third coordinate of the interaction point. At present knowldege of this third coordinate is limited to the thickness of the scintillator, that is, 3 mm. If interaction points are distributed uniformly with z, and we assume the value of z to be always in the middle of the crystal, then this will lead to an overall average error in the 3-D POI of around 1 mm.

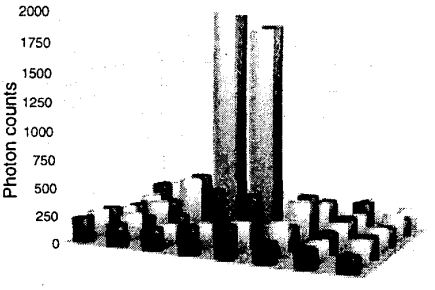

Figure 6: Distribution of detected photons for interaction point in middle of scintillator and 2.7 mm from detector surface

V. References

[1] B. E. Patt, J. S. Iwanczyk, C. Rossington, et al., "High Resolution CsI(Tl)/Si-PIN Detector Development for Breast Imaging," *IEEE Trans. Nucl. Sci.* vol 45, August 1998, pp. 2126-2131.

[2] W. W. Moses and S. E. Derenzo, "Design Studies for a Pet Detector Module Using a PIN Photodiode to Measure Depth of Interaction" *IEEE Trans. Nucl. Sci.* vol 41, August 1994, pp. 1441-1445.

[3] Shi Yin, T. O. Tumer, D. Maeding et al., "Hybrid Direct Conversion Detectors for Digital Mammography" *IEEE Trans. Nucl. Sci.* vol 46, December 1999, pp. 2093-2097.

[4] O. Toker, S. Masciocchi, E. Nygard et al., "VIKING, a CMOS Low Noise Monolithic 128 Channel Frontend for Si-strip Detector Readout" *Nucl. Instr. and Meth. in Phys. Res. A* vol 340, 1994, pp. 572-579.

[5] M. Moszynski, M. Kapusta, M. Mayhugh et al., "Absolute Light Output of Scintillators" *IEEE Trans. Nucl. Sci.* vol 44, June 1997, pp. 1052-1061.

[6] S. Siegel, S. R. Cherry, A. R. Ricci et al., "Development of Continuous Detectors for a High Resolution Animal PET System" *IEEE Trans. Nucl. Sci.* vol 42, August 1995, pp. 1069-1074.

[7] M. L. F. Lerch, A. B. Rosenfeld, P. E. Simmonds, et al., "Spectral Characterisation of a Blue Enhanced Silicon Photodector" *IEEE NSS/MIC 2000 Conference Record* submitted.

[8] J. Bea, A. Gadea, L. M. Garcia et al., "Simulation of Light Collection in Scintillators with Rough Surfaces" *Nucl. Instr. and Meth. in Phys. Res. A* vol 350, 1994, pp. 184-191.

[9] G. F. Knoll, T. F. Knoll and T. M. Henderson, "Light Collection in Scintillation Detector Composites for Neutron Detection" *IEEE Trans. Nucl. Sci.* vol 35, February 1988, pp. 872-875.

[10] A. Levin and C. Moisan, "A More Physical Approach to Model the Surface Treatment of Scintillation Counters and its Implementation into DETECT" *1996 IEEE Nuclear Science Symposium Conference Record 2* 1997, pp. 702-706.